Characterization of the First α-(1→3) Branching Sucrases of the GH70 Family*[S]

Marlène Vuillemin, Marion Claverie, Yoann Brison, Etienne Séverac, Pauline Bondy, Sandrine Morel,
Pierre Monsan, Claire Moulis[1], and Magali Remaud-Siméon[2]

From the Université de Toulouse, Institut National des Sciences Appliquées (INSA), Université Paul Sabatié (UPS), Institut National Polytechnique (INP), Laboratoire d'Ingénieries des Systèmes Biologiques et des Procédés (LISBP), 135 Avenue de Rangueil, F-31077 Toulouse, France, CNRS, UMR5504, F-31400 Toulouse, France, and Institut National de la Recherche Agronomique (INRA), UMR792 Ingénierie des Systèmes Biologiques et des Procédés, F-3140 Toulouse, France

Leuconostoc citreum **NRRL B-742 has been known for years to produce a highly α-(1→3)-branched dextran for which the synthesis had never been elucidated. In this work a gene coding for a putative α-transglucosylase of the GH70 family was identified in the reported genome of this bacteria and functionally characterized. From sucrose alone, the corresponding recombinant protein, named BRS-B, mainly catalyzed sucrose hydrolysis and leucrose synthesis. However, in the presence of sucrose and a dextran acceptor, the enzyme efficiently transferred the glucosyl residue from sucrose to linear α-(1→6) dextrans through the specific formation of α-(1→3) linkages. To date, BRS-B is the first reported α-(1→3) branching sucrase. Using a suitable sucrose/dextran ratio, a comb-like dextran with 50% of α-(1→3) branching was synthesized, suggesting that BRS-B is likely involved in the comb-like dextran produced by *L. citreum* NRRL B-742. In addition, data mining based on the search for specific sequence motifs allowed the identification of two genes putatively coding for branching sucrases in the genome of *Leuconostoc fallax* KCTC3537 and *Lactobacillus kunkeei* EFB6. Biochemical characterization of the corresponding recombinant enzymes confirmed their branching specificity, revealing that branching sucrases are not only found in *L. citreum* species. According to phylogenetic analyses, these enzymes are proposed to constitute a new subgroup of the GH70 family.**

Numerous lactic acid bacteria from the *Leuconostoc* genus isolated from different habitats, such as sugar juice, fermenting vegetables, or dairy products, have long been known to produce slimes in sucrose solution (1, 2). These slimy compounds were rapidly characterized as dextrans, homopolymers of α-D-glucopyranosyl units mainly linked by α-(1→6) linkages. Dextrans with a high content of α-(1→6) linkages and a low degree of branching found their first industrial applications in the 1940s

as a source of synthetic blood volume expanders (3). These findings motivated Jeanes *et al.* (22) to investigate the diversity of polymers produced during sucrose fermentation by different strains of lactic acid bacteria. A total of 96 strains were screened, and their dextrans were structurally characterized. In this study one strain, *Leuconostoc mesenteroides* NRRL B-742, also known as *L. mesenteroides* ATCC 13146 and renamed *Leuconostoc citreum* NRRL B-742 (4), received particular attention. Indeed, this strain, first isolated from a can of spoiled tomatoes in 1927 (1), was shown to produce two types of dextrans that differed by their structures and degree of solubility from sucrose. The less soluble polymer contained 75% of α-(1→6) linkages and 15% of α-(1→4) linkages, whereas the more soluble polymer displayed an uncommon comb-like structure consisting of a linear backbone of α-(1→6)-D-glucopyranosyl residues grafted with one α-(1→3)-linked glucosyl unit on every glucosyl moiety (5–9). Concomitantly with those findings, dextrans were shown to be synthesized by α-transglucosylases, commonly named glucansucrases, and today classified in the family 70 of glycoside hydrolases (GH70)[3] (10). The GH70 family belongs to the clan GH-H, together with families GH13 and GH77. To date, 279 α-transglucosylase sequences have been reported in the CAZy database, and only 25% has been functionally characterized (11). Furthermore, only four three-dimensional structures of GH70 enzymes have been solved (12–15). The enzymes are organized into five different structural domains, A, B, C, IV, and V. The A, B, and C domains are related to GH13 family enzymes, whereas domains IV and V are GH70-specific domains. The fold of these enzymes is unique, and except for domain C, all domains are formed by non-contiguous fragments of sequences that assemble around a U-turn (15). These enzymes are α-retaining enzymes. They mainly catalyze α-transglucosylation reactions through a classical double displacement mechanism. The reaction starts with the formation of a β-D-glucosyl-enzyme intermediate involving a nucleophilic aspartate, an acid-base glutamic acid, and a third aspartate that stabilizes the covalent intermediate. In a second step the intermediate can be intercepted by a water molecule (hydrolysis reaction) or by the hydroxyl group of an acceptor (transgluco-

---

[1] To whom correspondence may be addressed: INSA, LISBP, 135 Avenue de Rangueil, F-31077 Toulouse, France. Tel.: 33-561-559-446; Fax: 33-561-559-400; E-mail: moulis@insa-toulouse.fr.
[2] To whom correspondence may be addressed: INSA, LISBP, 135 Avenue de Rangueil, F-31077 Toulouse, France. Tel.: 33-561-559-446; Fax: 33-561-559-400; E-mail: remaud@insa-toulouse.fr.

[3] The abbreviations used are: GH, glycoside hydrolase; HPAEC-PAD, high performance anion exchange chromatography with pulsed amperometric detection; HPSEC, high performance size exclusion chromatography; contig, group of overlapping clones.

First α-(1→3) Branching Sucrases from the GH70 Family
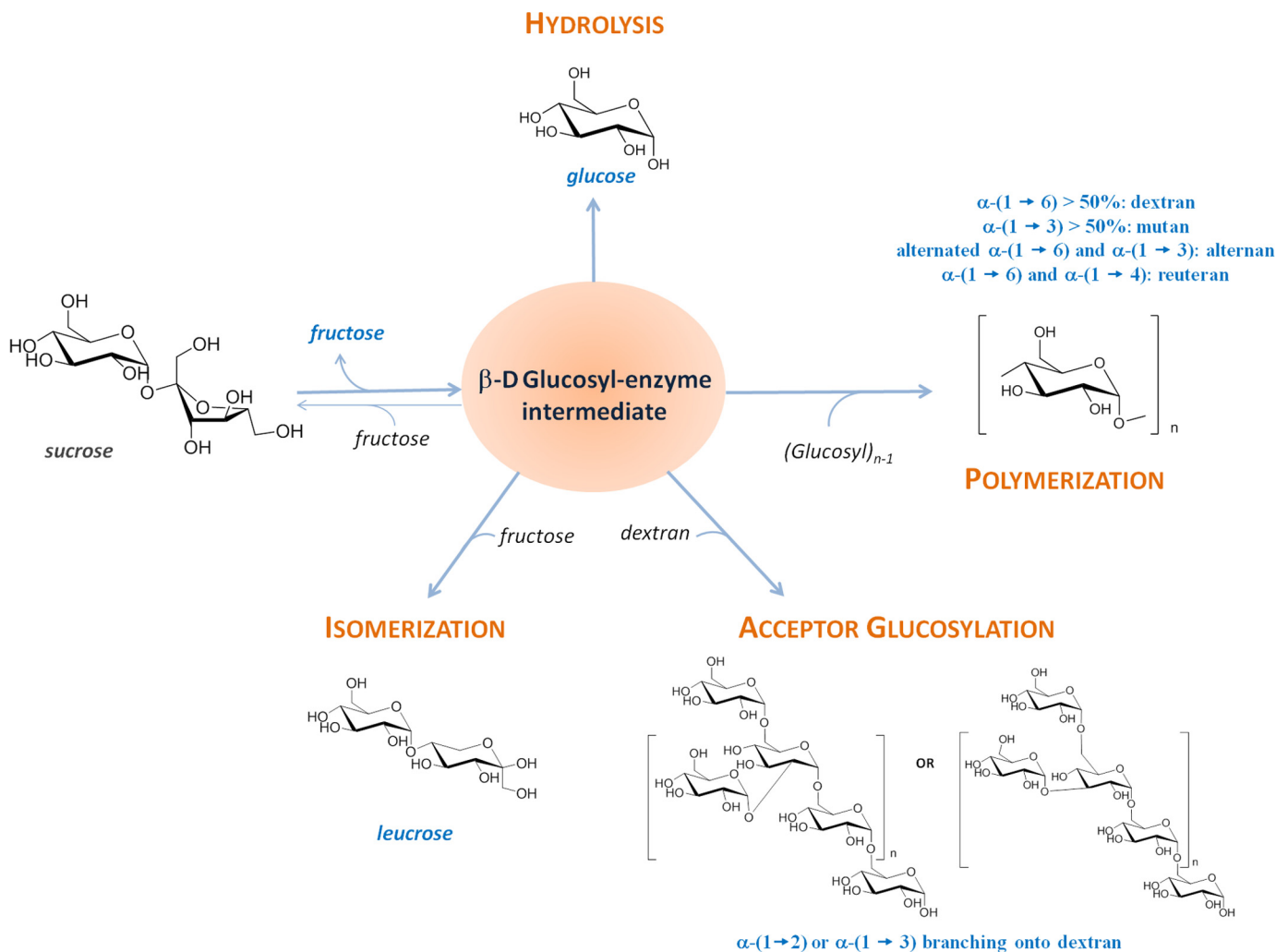
SCHEME 1. **Main reactions catalyzed by GH70 sucrose-active enzymes.**

sylation). The synthesis of the polymer occurs via successive transfers of glucosyl units onto the non-reducing extremity of the growing α-glucan chain (Scheme 1) (16–18).

Among GH70 sucrose-active enzymes, four subgroups of glucansucrases can be distinguished: the dextransucrases, alternansucrases, mutansucrases, and reuteransucrases, which are all efficient polymerases (10). In addition, one branching sucrase (GBD-CD2) was engineered from *L. citreum* NRRL B-1299 DSR-E dextransucrase (19). This enzyme displays no polymerase activity but catalyzes α-(1→6) dextran branching very efficiently with single α-(1→2)-linked glucosyl units (Scheme 1) (20). Recently, genome sequencing of *L. citreum* NRRL B-1299 allowed the identification of the first natural α-(1→2) branching sucrase, BRS-A, that shows the same specificity as GBD-CD2. This enzyme was proposed to be involved in the formation of the native dextrans of *L. citreum* NRRL B-1299 that contain a high percentage of α-(1→2) linkages (21, 22).

The formation of the regular hyper-branched dextran of *L. citreum* NRRL B-742 is even more intriguing. Several attempts to isolate the GH70 enzymes of *L. citreum* NRRL B-742 were reported. However, although the enzyme responsible for the production of dextran with both α-(1→6) and α-(1→4) linkages was isolated, the enzyme contributing to the comb-like structure was never identified (5). Of note, most of the GH70 enzyme activities were found strongly attached to the cell wall, making the enzymes difficult to purify (7). Crude enzyme extracts or sucrose fermentation broths were thus used to produce α-(1→3)-branched glucooligosaccharides from sucrose and maltose (7), and these compounds were shown to possess interesting functional properties. In particular, they stimulated *in vitro* growth of beneficial bacteria such as bifidobacteria or lactobacilli and inhibited the development of pathogens such as *Salmonella* sp. or *Escherichia coli* (23, 24). In 2000, Kim and Robyt (25) cloned a gene from the mutant strain *L. citreum* NRRL B-742CB. The encoded protein, DSR-B-742, shared >95% amino acid identity with DSR-B dextransucrase from *L. citreum* NRRL B-1299 and synthesized a quasilinear dextran with >95% of α-(1→6) linkages (26). Thus far the mode of synthesis of the comb-like dextran has remained unknown.

A genomic approach was undertaken to gain insight into the formation of this hyper-branched α-glucan and to have access to enzymatic tools of interest for functional glucooligosaccharide synthesis. First, the genome of *L. citreum* NRRL B-742 was sequenced (27) and mined to determine its content in GH70 α-transglucosylase encoding genes. One putative GH70 gene

TABLE 1
Primers, vectors, and strains used in this study and their main features

Primers		
Description	*Main features*	
5'-<u>CACC</u>ATGGAAATGAAAGAAACAATCACTCG-3'	Forward primer used to amplify *brsB* gene	
5'-AAGCTTGCAAAGCACGCTTATCAATC-3'	Reverse primer used to amplify *brsB* gene	
5'-<u>CACC</u>GATACACAAACGCCGGTTGGTACA-3'	Forward primer used to amplify *brsBΔ1* gene	
5'-GAGTTGTGTTGGTAGGCTATATTG-3'	Reverse primer used to amplify *brsBΔ1* gene	
5'-<u>CACC</u>ATGAAGCAGCAAGAGAGCATC-3	Forward primer used to amplify *brsC* gene	
5'-AAACGCACGTTTATCAATCCATAC-3'	Reverse primer used to amplify *brsC* gene	

Vectors		
Description	*Main features*	*Supplier*
pBAD-DEST49	Used for *brsB* expression N-terminal HP-Thioredoxin fusion C-terminal V5 and 6xHis tags	Life Technologies, Carlsbad, CA, USA
pET-55-DEST	Used for *brsBΔ1* expression N-terminal Strep Tag II tag C-terminal 6xHis tag	Merck Millipore, Darmstadt, Germany

Strains		
Description	*Main features*	*Supplier*
E. coli TOP10	Used for all cloning experiments	
E. coli BL21-AI	Used for BRS-B production	Life Technologies
E. coli BL21 star DE3	Used for BRS-B-Δ1 production	

showing divergence from various consensus sequences of GH70 family enzymes was cloned for recombinant expression in *E. coli*. The corresponding protein, named BRS-B, is an α-(1→3) branching sucrase. A shorter version of BRS-B, named BRS-B-Δ1, was rationally designed and characterized. The specificity of BRS-B and its truncated form was investigated and revealed the interest of these enzymes for the production of α-(1→3)-branched dextrans with a controlled degree of branching. In addition, comparison of these enzymes with the recently discovered α-(1→2) branching sucrase (BRS-A) allowed the identification of two enzymes in public databases that were found to catalyze dextran branching and were clustered with previously characterized branching sucrases in the GH70 phylogenetic tree.

Experimental Procedures

Isolation of brsB Gene and Analysis of BRS-B Primary Structure

The *brsB* gene was identified in the *L. citreum* NRRL B-742 genome (27) (NCBI reference sequence: NZ_CCNG01000013.1) by performing a nucleotide BLAST against a homemade GH70 α-transglucosylase-encoding gene database. The protein sequence of BRS-B is deposited under the GenBank™ accession number CDX65123.1. Protein sequence comparison was performed either using protein Blast (NCBI) against the non-redundant protein sequence database (nr) for local alignments or using Clustal Omega for global alignments with other GH70 enzymes. Protein sequence global alignment with GTF-180-ΔN glucansucrase (15) and ΔN₁₂₃-GBD-CD2 (12) was used to determine length and position of domains A, B, C, IV,

and V. The signal peptide cleavage was predicted using SignalP 4.1 server.

Isolation of Genomic DNA

L. citreum NRRL B-742 was grown on 1.5 ml of MRS medium (Sigma-Aldrich) at 30 °C overnight. Genomic DNA was isolated using the Wizard® genomic DNA purification kit (Promega, Madison, WI) according to the supplier's recommendations for Gram-positive bacteria.

Cloning of brsB and brsBΔ1 Genes

The gene *brsB* and a truncated form lacking the signal peptide and the last 575 amino acids at the C terminus of the protein (*brsBΔ1*) were amplified by PCR from *L. citreum* NRRL B-742 genomic DNA template. The primers used are described in Table 1. The addition of the CACC sequence (underlined) to the 5'-forward primers allowed the correct insertion of the genes into the pENTR/D-TOPO® vector (Life Technologies). From a positive entry clone, LR recombination (Gateway® LR Clonase® II enzyme mix, Life Technologies) was performed using the destination vectors described in Table 1. Expression clones were selected on LB agar plates supplemented with 100 μg ml⁻¹ of ampicillin. Plasmids were extracted with the Sigma GenElute HP Plasmid Miniprep kit, verified by restriction analyses and sequencing (GATC Biotech, Constance, Germany).

Recombinant Production of BRS-B and BRS-B-Δ1

Starter Culture—*E. coli* BL21-AI and *E. coli* BL21 star DE3 cells (detailed in Table 1) were freshly transformed by pBAD-

49/*brsB* and pET-55/*brsBΔ1*, respectively. Thirty milliliters of LB medium, supplemented with ampicillin (100 μg ml^{-1}), were inoculated with 200 μl of transformation mix and incubated overnight at 37 °C under agitation (200 rpm).

Erlenmeyer Flask Cultures—One liter of modified ZYM5052 medium (28) contained (i) 0% lactose, 0% glucose, 0.5% glycerol and 0.01% L-arabinose for BRS-B production or (ii) 0.1% lactose, 0% glucose and 1% glycerol for BRS-B-Δ1 production. Both were supplemented with ampicillin (100 μg ml^{-1}) and were inoculated with the corresponding starter culture at an $A_{600\,nm}$ of 0.05. Cultures were incubated at 21 °C under agitation (150 rpm). After a 26-h incubation, cells were harvested by centrifugation, dispersed in 50 mM sodium acetate buffer, pH 5.75, at a final $A_{600\,nm}$ 80 and disrupted by sonication. The recombinant enzymes were recovered in the soluble fraction after centrifugation (15,000 × g, 30 min, 4 °C) of the crude cell extract.

Affinity Chromatography Purification of Enzymes

All purification assays were performed using the ÄKTAxpress (GE Healthcare) at 12 °C. For His$_6$ tag affinity chromatography, cells were centrifuged and resuspended in binding buffer (20 mM phosphate sodium buffer, pH 7.4, 500 mM NaCl, 20 mM imidazole, 2.5% (v/v) glycerol) at a final $A_{600\,nm}$ of 200. After disruption by sonication, centrifugation (30,000 × g, 30 min, 4 °C), and filtration through a 0.22-μm cartridge (Sartorius Stedim Biotech, Aubagne, France), lysates were applied onto a 1-ml HisTrap HP® column (GE Healthcare) that had been equilibrated with the binding buffer. The proteins were eluted by an imidazole gradient from 10 to 500 mM over 25 min. Eluate fractions of 3 ml were desalted onto a 10-DG column (Bio-Rad) with 50 mM sodium acetate buffer at pH 5.75 with 100 mM NaCl, 0.05 g liter^{-1} CaCl$_2$, and 0.1% (v/v) Tween 80. In order to remove small contaminants, purified eluates were washed 3 times onto Vivaspin 2 with a molecular weight cut-off of 100 (Sartorius Stedim Biotech).

Enzymatic Activity Assay

One unit of BRS-B, BRS-B-Δ1, BRS-C, or BRS-D is defined as the amount of enzyme that catalyzes the production of 1 μmol of fructose/min at 30 °C in 50 mM sodium acetate buffer at pH 5.75 from 292 mM sucrose. The enzyme activities were determined by measuring the amount of reducing sugars using the dinitrosalicylic acid method (29).

pH and Temperature Optima; Effect of Divalent Ions

Optimal pH and temperature were determined in duplicate using 1 unit·ml^{-1} of enzyme in the presence of 292 mM sucrose and 119 mM dextran (68,400 g·mol^{-1}) for both BRS-B (in sonicated extract) and the pure BRS-B-Δ1. To evaluate the optimal pH, the assays were performed at 30 °C in 50 mM citrate phosphate buffer with pH values varying from 3.5 to 7.0 in increments of 0.5 units. Optimal temperature was determined from assays carried out in 50 mM sodium acetate buffer at pH 5.75 at temperatures of 23, 26, 30, 33, 37, 40, or 45 °C. The effect of salts on transferase activity of BRS-B-Δ1 was determined by incubating the enzyme (1 unit·ml^{-1}) with 1 mM EDTA to trap the possible presence of any divalent ion in the catalytic core of the enzyme or with 1 mM CaCl$_2$, CuCl$_2$, ZnCl$_2$, or MgCl$_2$ salts. Activity assays were performed at 30 °C in 50 mM sodium acetate buffer, pH 5.75, 292 mM sucrose, and 119 mM of dextran (68,400 g·mol^{-1}). For all these experiments, the enzymatic activity was determined by measuring fructose release by high performance liquid chromatography (HPLC) on a Dionex system and using an Aminex® HPX-87K carbohydrate analysis column (300 × 7.8 mm; Bio-Rad). Column oven temperature was set at 65 °C, and ultrapure water was used as eluent (0.6 ml min^{-1}).

Determination of BRS-B-Δ1 Kinetic Parameters

Reaction with Sucrose—Kinetic parameters with sucrose as the sole substrate were determined in 50 mM sodium acetate buffer at pH 5.75 supplemented with 250 μg ml^{-1} bovine serum albumin, 23 μg ml^{-1} of purified BRS-B-Δ1 at 30 °C and using initial sucrose concentrations ranging from 3 to 600 mM. All initial velocities were measured by quantifying fructose release at the early stage of reaction (when <5% of the substrate is consumed and when leucrose and other oligosaccharide production can be neglected). At regular time intervals samples were withdrawn and immediately heated at 95 °C for 5 min to stop the reaction. Fructose concentration was determined by HPLC as described above. K_m, K_i, and V_{max} parameters were determined using SigmaPlot Kinetics software and fitted to a non-competitive substrate inhibition model.

α-(1→3) Transglucosylation—Kinetic parameters for α-(1→3) transglucosylation were determined at 30 °C in 50 mM sodium acetate buffer, pH 5.75, supplemented with 250 μg ml^{-1} BSA, 9.5 mg liter^{-1} of enzyme, 300 mM sucrose, and dextran of 68,400 g·mol^{-1} at final concentrations ranging from 31 to 617 mM. For the sake of clarity, dextran concentrations will be expressed as molar concentrations of anhydroglucosyl units within the dextran, as determined by dividing dextran mass concentrations by 162 g·mol^{-1}. All initial velocities were measured when <5% of the sucrose was consumed. Initial α-(1→3) transglucosylation velocities were calculated by subtracting fructose (representing the total activity) by free glucose (representing hydrolase activity) production rates. Glucose and fructose concentrations were determined by HPLC using the same conditions as those described previously. $K_{m\,dextran}$ and V_{max} were estimated using SigmaPlot Kinetics software and fitted to a Michaelis-Menten model.

Synthesis of α-(1→3)-branched Dextrans Using BRS-B and BRS-B-Δ1

Various α-(1→6)-linked dextrans of average molar masses ranging from 1500 to 2 × 10^6 g·mol^{-1} (Sigma) were incubated at different concentrations with sucrose (9–438 mM) using 1 unit·ml^{-1} BRS-B (or BRS-B-Δ1) at 30 °C in 50 mM sodium acetate buffer at pH 5.75 for 8–16 h. Reactions were stopped by a 5-min incubation at 95 °C. The various tested sucrose/dextran ratios are reported in supplemental Table S1.

HPAEC-PAD Analysis

To determine production yield and assay sucrose depletion, reaction media were analyzed by HPAEC-PAD (high performance anion exchange chromatography with pulsed ampero-

metric detection) using a CarboPac™ PA100 (4 × 250 mm) analytical column coupled with a CarboPac™ PA-100 guard (4 × 50 mm). Glucose, fructose, leucrose, and sucrose were separated using a 30-min sodium acetate gradient from 6 to 300 mM in 150 mM NaOH. The amount of each sugar was determined using standards of 5, 10, 15, and 20 mg kg^{-1}. Samples were prepared in ultra-pure water and diluted to a final concentration of 10–15 mg kg^{-1} of total sugars for quantitative analyses and a final concentration of 250 mg·kg^{-1} (total sugars) for qualitative analyses. The percentage of glucosyl units from sucrose incorporated into glucose (%G$_{glucose}$) or leucrose (%G$_{leucrose}$) was calculated as follows.

$$\%G_{glucose} = \frac{([glucose]tf - [glucose]t0) \times 342}{([sucrose]t0 - [sucrose]tf) \times 180} \times 100$$

(Eq. 1)

$$\%G_{leucrose} = \frac{([leucrose]tf - [leucrose]t0)}{([sucrose]t0 - [sucrose]tf)} \times 100$$ (Eq. 2)

High Performance Size Exclusion Chromatography (HPSEC) Analysis

HPSEC analyses were carried out using Shodex OH-Pak SB-802.5 and SB-805 columns in series coupled with a Shodex OH-Pak SB-G guard column and placed in an oven at 70 °C. Elution was performed using 0.45 M NaNO$_3$ and 1% ethylene glycol (v/v) as the eluent using a flow rate of 0.3 ml min^{-1}. The samples were diluted at 10 g kg^{-1} of total sugars and also in 0.45 M NaNO$_3$ and 1% ethylene glycol.

The percentage of glucosyl units from sucrose incorporated into α-(1→3)-branched dextran was calculated as,

$$\%G_{dextran} = \frac{Area_{dextran} \times 342}{Area_{sucrose} \times 162}$$ (Eq. 3)

The percentage of glucosyl units from sucrose incorporated into small oligosaccharides was deduced as,

$$\%G_{small\ oligosaccharides} = 100\% - (\%G_{dextran} + \%G_{glucose}$$
$$+ \%G_{leucrose})$$ (Eq. 4)

Here %G$_{dextran}$, %G$_{glucose}$, and %G$_{leucrose}$ have been determined from HPSEC and HPAEC-PAD analyses.

^{1}H and ^{13}C NMR Analysis of Oligosaccharides and Polymers

To determine α-(1→3) linkage content, freeze-dried polymer samples were dispersed in deuterated water at a final concentration of 20 mg ml^{-1}. NMR spectra were recorded on an Advance 500 MHz spectrometer (Bruker) operating at 500 MHz for ^{1}H NMR and 125 MHz for ^{13}C using a 5-mm z-gradient TBI probe. The data were processed using TopSpin 3 software. One-dimensional ^{1}H NMR spectra was acquired by using a zgpr pulse sequence (with water suppression). All measurements were performed at 298 K, and chemical shifts were referenced to an internal reference sodium 2,2,3,3-tetradeutero-3-trimethylsilylpropanoate (^{1}H = 0 ppm) and acetone (^{13}C = 31.08 ppm). The percentages of α(1→3) and α(1→6) linkages in

α-glucans were calculated by integrating the corresponding anomeric proton signals (30).

Model Construction

Sequence alignment between BRS-B (from residues Ile-220 to Ile-1300) and ΔN123-GBD-CD2 was generated using MUSCLE (31). This alignment was checked, locally corrected in variable loop regions, and submitted to SWISS-MODEL online service for protein structure prediction using the alignment mode (32). The same procedure was applied for the sequence of BRS-A (from residues Gly-223 to Val-1289). BRS-B and ΔN123-GBD-CD2 share 53% sequence identity; BRS-A and ΔN123-GBD-CD2 share 60% sequence identity. All drawings were realized using PyMOL software (DeLano Scientific).

Identification of New Branching Sucrases

Blast analysis (blastp and blastn) were performed to identify new putative branching sucrases in NCBI public databases. The putative proteins displaying similarities with characterized branching sucrases (*i.e.* BRS-A, BRS-B, and/or GBD-CD2) were selected considering that the sequence should display (i) one phenylalanine at subsite +1 (position 675, BRS-B numbering), (ii) a non-aromatic residue at subsite +1 (position 711, BRS-B numbering), (iii) one isoleucine at position 783 (BRS-B numbering), (iv) one histidine at position 785 (BRS-B numbering), (v) one lysine at position 789 (BRS-B numbering), and (vi) one valine at position 795 (BRS-B numbering).

Cloning of the brsC Gene

First, a synthetic *brsC* gene (contig GenBank™ accession number AEIZ01000002, positions 68,715–63,391 on reverse strand) was designed to optimize its expression in *E. coli* (GeneCust, Dudelange, Luxembourg). The gene was then amplified by PCR from pUC57/*brsC* plasmid DNA template using the primers described in Table 1. The PCR product was then inserted into the pENTR/D-TOPO vector (Life Technologies). From a positive entry clone, LR recombination (Gateway LR Clonase II enzyme mix; Life Technologies) was performed with the pET-55-DEST destination vector (Merck Millipore). Expression clones were selected on LB agar plates supplemented with 100 μg ml^{-1} of ampicillin. Plasmids were then extracted using the GenElute HP Plasmid Miniprep kit (Sigma), verified by restriction analyses, and sequenced (GATC Biotech). *E. coli* TOP10 competent cells (Life Technologies) were used for all cloning experiments.

Recombinant Production of BRS-C and BRS-D Branching Sucrases

The construction pET28b/*brD* was provided by Biomatik (Cambridge, ON, Canada) where the *brsD* gene (GenBank™ accession number AZBY01000038.1, locus tag LAKU_38c00010) was designed to optimize the heterologous expression in *E. coli*.

Starter Culture—*E. coli* BL21 star DE3 cells were freshly transformed by pET-55/*brsC,* pET28b/*brD.* 30 ml of LB medium supplemented with ampicillin (100 μg ml^{-1}) were inoculated with 200 μl of transformation mix and incubated overnight at 37 °C under agitation (200 rpm).
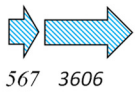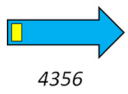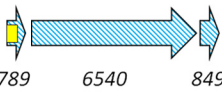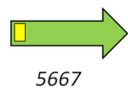
First α-(1→3) Branching Sucrases from the GH70 Family
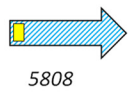
	dsrA-like	dsrB-742	dsrE-like	brsB	dsrF-like
ORF	567 3606	4356	789 6540 849	5667	5808
Blastn (best blast hit)	99% id *dsrA* Ln. citreum NRRL B-1299	-	99% id *dsrE* Ln. citreum NRRL B-1299	76% id brsA Ln. citreum NRRL B-1299	99% id *dsrF* Ln. citreum B110-1-2
Specificity	Dextransucrase (Putative)	Dextransucrase (Characterized)	Dextransucrase (Putative)	Characterized herein	Dextransucrase (Putative)

FIGURE 1. **GH70 encoding genes in *L. citreum* NRRL B-742 genome**. *Yellow squares* represent putative signal peptide encoding sequences. *Hatched arrows* indicate sequences showing >99% identity with previously characterized glucansucrases. The *solid blue arrow* indicates the gene previously characterized dsrB-742 (26). The *green arrow* stands for the *brsB* gene characterized in this study. *Numbers below the arrows* correspond to the size of the ORF in bp. The enzyme specificity was predicted according to sequence homology with other characterized GH70 enzymes.
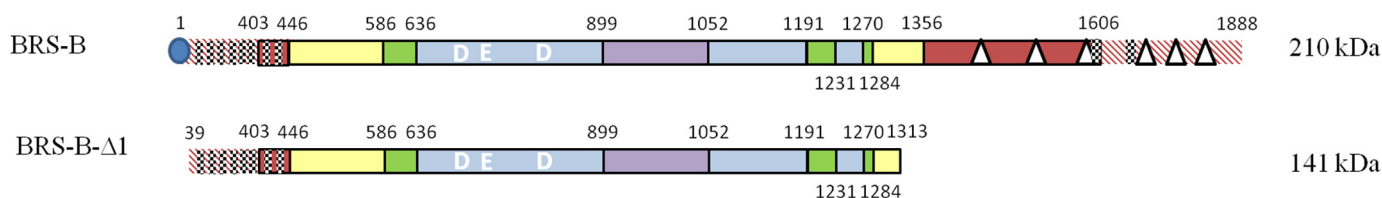

FIGURE 2. **Schematic representation of the structural organization of BRS-B.** The five different structural domains were assigned by comparison with those of GTF180-ΔN and ΔN$_{123}$-GBD-CD2: (i) domain V in *red*), (ii) domain IV in *yellow*, (iii) domain B in *green*, (iv) domain A in *blue*, and (v) domain C in *purple*. The catalytic residues (*DED*) are indicated in *bold* and *white*, YG repeats (36) with *checkered red* motifs and APY repeats (39) with *white triangles*. Signal peptide is represented by a *blue circle*. The *red hatched regions* correspond to zones for which no structural information is available.

Erlenmeyer Flask Cultures—1 liter of modified ZYM5052 medium (28) (with the changes 0.1% lactose, 0% glucose, and 1% glycerol, supplemented with ampicillin (100 μg ml^{-1}) was inoculated with the starter culture at an $A_{600\,nm}$ of 0.05. Cultures were incubated at 21 °C under agitation (150 rpm). After 26 h of incubation, cells were harvested by centrifugation, resuspended in 50 mM sodium acetate buffer, pH 5.75, at a final $A_{600\,nm}$ of 80, and disrupted by sonication. Recombinant enzymes were recovered after centrifugation (15,000 × g, 30 min, 4 °C) in the soluble fraction of the crude cell extract.

Phylogenetic Analysis

A phylogenetic tree was constructed from 60 protein sequences, including the functionally characterized GH70 enzymes indexed in the CAZY database and the branching sucrases BRS-A, BRS-B, BRS-C, BRS-D, and GBD-CD2. Protein sequences were aligned using Clustal Omega. GBlock program was used to remove highly variable regions. A total of 1371 positions (42%) were then conserved. The tree was constructed using the Neighbor-joining method using the SeaView 4.5.4 software. The percentage of replicate trees in which the associated taxa clustered together in the bootstrap test (100 replicates) is shown next to the branches. The tree is drawn to scale, with branch lengths in the same units as those of the evolutionary distances used to infer the phylogenetic tree. The evolutionary distances were computed using the Poisson correction method and are in the units of the number of amino acid substitutions per site. The tree was displayed using FigTree v1.4.2 software.

Results and Discussion

Characterization of a Novel GH70 Branching Sucrase from L. citreum NRRL B-742—The analysis of *L. citreum* NRRL B-742 genome (27) revealed the presence of five putative α-transglucosylase encoding genes: (i) the *dsrB-742* gene previously isolated by Kim *et al.* (26), (ii) three additional genes, *dsrA*-like, *dsrE*-like, and *dsrF*-like, that share 99% identity with the characterized dextransucrase genes from *L. citreum* NRRL B-1299 and B110-1-2 (33–35), and (iii) one gene of 5667 bp, named *brsB*, putatively encoding a 1888-amino acid protein showing 76% of amino acid identity and 83% of similarity with BRS-A from *L. citreum* NRRL B-1299 (21) (GenBank^{TM} accession number WP_040177263.1, best Blast hit against the non-redundant (nr) protein database) (Fig. 1).

For BRS-B, a signal peptide with a cleavage site between positions 39 and 40 was predicted using SignalP 4.1 server. Based on sequence alignment, the protein was predicted to belong to the GH70 enzyme family and to adopt the same structure as those displayed by other GH70 enzymes (12–14), which consist of five structural domains A, B, C, IV, and V, of which the limits were assigned by comparison with those of GTF180-ΔN and ΔN$_{123}$ GBD-CD2 (12, 15) (Fig. 2). The three catalytically important amino acids involved in the formation of the β-D-glucosyl-enzyme intermediate are conserved in the BRS-B sequence and are located in catalytic domain A. By analogy with other GH70 α-transglucosylases, Asp-671, Glu-709, and Asp-788 residues are predicted to play the role of the nucleophile, the acid/base catalyst, and the transition state stabilizer, respectively. Domain V is formed by two fragments, one at the N terminus and

the other at the C-terminal extremity of the protein, and is predicted to constitute both extremities of the U-shape fold (15). Like most of the domains V of GH70 enzymes, this domain is rich in YG repeats that were previously suggested to play a key role in interactions between glucansucrases and their polymers (36). Eight and two YG repeats that could be involved in α-glucan binding were identified at the N- and C-terminal extremities, respectively (Fig. 2). Additionally, at the C terminus, 6 APY repeats were identified and shared 99% of identity with those found at the C-terminal ends of the alternansucrase (ASR) from *L. citreum* NRRL B-1355 and the branching sucrase BRS-A from *L. citreum* NRRL B-1299 (513 out of 518 amino acids) (37, 38). The APY repeats of alternansucrase (ASR) were previously deleted without causing any alteration of enzyme activity or specificity (39).

The *brsB* gene was cloned into pBAD-DEST49 vectors and expressed in *E. coli* BL21-AI host strain to characterize the corresponding protein. The level of production reached 700 units·liter^{-1} of culture. Western blot analyses confirmed that the full-length BRS-B was the most abundant protein, even if slightly degraded forms could also be observed (data not shown).

As the native *E. coli* BL21-AI does not produce any sucrose-active enzymes, the sonication extract was used to characterize the catalytic activities of BRS-B. The optimal temperature and pH were estimated at 30–33 °C and pH 5.5–6 (data not shown). All subsequent assays were thus performed at 30 °C and at pH 5.75. Enzymatic reactions were first carried out in the presence of 292 mM sucrose, the natural substrate for most of GH70 enzymes. The main reaction products formed were glucose and leucrose (*O*-α-D-glucopyranosyl-(1→5)-D-fructopyranose). A total of 51% of the glucosyl units from sucrose were incorporated into leucrose, and 33% were transferred onto water (hydrolysis reaction). The remaining part, representing 16% of the transferable glucosyl units, was incorporated into various small size glucooligosaccharides, which were not isolated and characterized due to their very low level of production (supplemental Fig. S1). No trace of high molar mass α-glucans was detected using HPSEC-RI, indicating that BRS-B is not an efficient polymerase.

Acceptor reactions were carried out using 1500 g·mol^{-1} dextran as the acceptor (66.6 mM) and sucrose as the donor (292 mM). As seen on HPAEC-PAD chromatograms, the product profile rapidly changed during the course of the reaction (Fig. 3a). The intensity of the peaks corresponding to linear isomaltooligosaccharides decreased, whereas new signals were clearly visible. The products synthesized after total sucrose depletion were analyzed by NMR spectroscopy. The ^{1}H NMR spectrum showed two peaks assigned to anomeric resonances at 4.99 ppm and 5.33 ppm, which correspond to the anomeric proton of a glucosyl unit engaged in α-(1→6) or α-(1→3) linkages, respectively. Integration of the anomeric signals showed that the amount of α-(1→3) linkages in dextran reached 39% that of the total osidic linkages (Fig. 3b). These results demonstrate that BRS-B catalyzes the transglucosylation reaction from sucrose onto dextran acceptors through the formation of α-(1→3) linkages.

Several dextrans of higher molar mass between 39,100 g·mol^{-1} and 2×10^{6} g·mol^{-1} were also tested as acceptors. All of them were efficiently branched by BRS-B, as evidenced by the percentage of α-(1→3) linkages reaching a maximum of 50%, indicating that each glucosyl moiety of the α-(1→6) backbone chain was substituted by an α-(1→3)-linked glucosyl residue (Fig. 4a).

The J-Mod spectrum of the dextran shows two anomeric ^{13}C chemical shifts at 98.63 ppm and 100.30 ppm corresponding to the ^{1}H anomeric signals at 4.98 ppm and 5.33 ppm of the α-(1→6) and α-(1→3)-linked glucosyl units, respectively. The presence of α-(1→3)-linked branching was further attested by the typical signal at 81.37 ppm, which was assigned to C-3 of the 3,6-*O*-disubstituted glucopyranosyl units (9, 40). Only one type of resonance is observed at 100.30 ppm, indicating that the α-(1→3) linkages of the dextran are solely branching linkages. This is confirmed by the presence of only one chemical shift at 61.20 ppm attributed to free C6. At 66.33 ppm, the resonances are attributed to bound C6 of the 3,6-*O*-disubstituted and 6-*O*-disubstituted glucosyl units of the main chain (Fig. 4b).

To date, BRS-B is the first reported α-(1→3) branching sucrase. Its ability to branch high molar mass dextran up to 50% suggests that BRS-B is likely involved in the synthesis of *L. citreum* NRRL B-742 comb-like dextran. Based on sequence alignment, the other putative GH70 enzymes encoded by *L. citreum* NRRL B-742 are predicted to be dextransucrases synthesizing linear dextrans. Dextransucrase activities were previously isolated in the fermentation broth of *L. citreum* NRRL B-742 (5, 22, 26). It can thus be assumed that the synthesis of the hyper-branched dextran is due to the synergistic action of at least one dextransucrase and the branching enzyme, BRS-B. The dextransucrase would synthesize the α-(1→6) backbone, and the α-(1→3) branching sucrase would be involved in branching via α-(1→3) osidic bond formation. There are several questions that remain, including understanding which dextransucrases of *L. citreum* NRRL B-742 work in tandem with BSR-B. Additionally, it is not known whether or not elongation and branching are concomitant. These pending questions require additional experiments, such as RT-quantitative PCR studies, secretome analysis at regular intervals of the culture, and knock-out of either polymerases or branching sucrase encoding genes combined with structural analyses of the produced dextran.

*Construction of BRS-B-Δ1, a Truncated Form of BRS-B—*Despite several attempts, the purification of BRS-B did not give satisfying results due to very weak protein binding onto nickel and cobalt affinity resins. This was attributed to an inadequate exposure of the tags, which could prevent correct interaction with the resin. To facilitate the purification process, a shorter form deleted of the signal peptide and all APY motifs at the C-terminal end, was constructed (Fig. 2). Notably, 8 of the 10 identified YG repeats were conserved. The position of the truncations at the C- and N terminus ends were determined from sequence alignment with the α-(1→2) branching sucrase ΔN$_{123}$ GBD-CD2. The production of the truncated protein BRS-B-Δ1 was optimized to a level of 1200 units·liter^{-1} using pET-55-DEST and BL21 Star DE3 *E. coli* strain. Western blot analysis showed that the protein was not degraded at the N-terminal
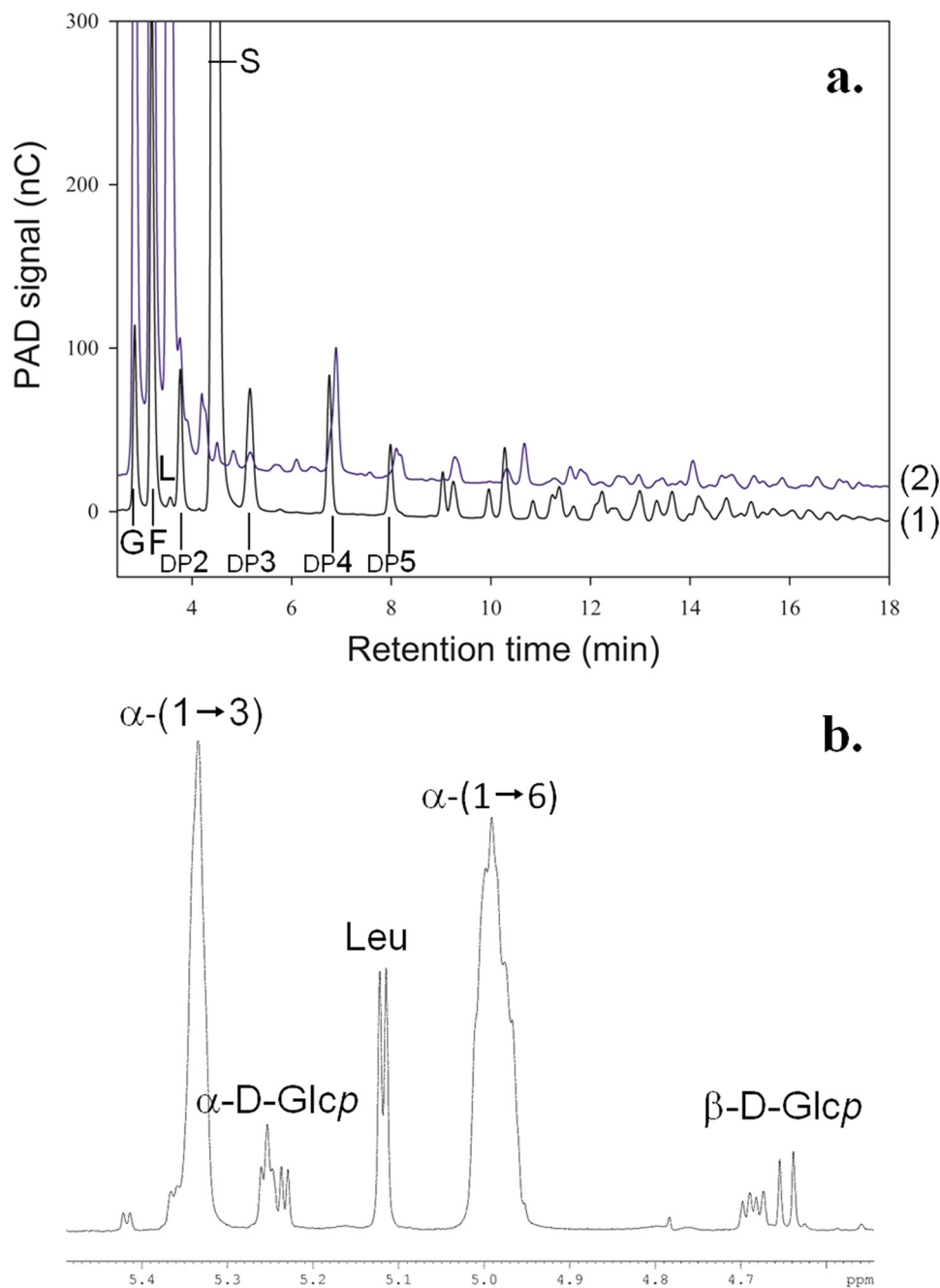
FIGURE 3. **Analysis of the products synthesized with BRS-B enzyme from sucrose (292 mM) and dextran 1500 g·mol^{-1} (66.6 mM).** *a*, HPAEC-PAD chromatograms of enzymatic reaction stopped after 1 min (*1*) and enzymatic reaction stopped after 8 h (*2*). Peaks corresponding to glucose (*G*), fructose (*F*), leucrose (*L*), sucrose (*S*), and isomaltooligosaccharides with a degree of polymerization (*DP*) of *x*. *b*, ^{1}H NMR spectrum (in the anomeric region) of the products synthesized by BRS-B at 500 MHz in D$_2$O. *Leu*, leucrose; *α-D-Glcp*, α-D-glucose; *β-D-Glcp*, β-D-glucose.

extremity. The C-terminal His$_6$ tag was then used to purify the enzyme onto Ni-NTA affinity resin. The purification yield reached 85%, with a corresponding purification factor of 17. BRS-B-Δ1-specific activity on sucrose (292 mM) was estimated at 24 units·mg^{-1} of protein. The optimal temperature and pH were determined to be between 33 and 40 °C and 5–5.75, respectively (Fig. 5, *a* and *b*) and are in the same range as those observed for the non-purified enzyme BRS-B. A slight improvement of transferase activity (near 6%) was observed with the addition of 1 mM Ca^{2+} (Fig. 5*c*), as previously described for the branching sucrase ΔN123-GBD-CD2 (increase of 13% (12)). In contrast, Zn^{2+} ions had the most deleterious effect on BRS-B-Δ1 activity, which decreased by 23% in the presence of Zn^{2+} ions (Fig. 5*c*). From a sucrose substrate, BRS-B-Δ1 showed a slightly higher hydrolytic activity than BRS-B and produced 42% glucose, 48% leucrose, and 10% of small oligosaccharides. The profiles of products obtained with dextran acceptors were similar to those obtained with the full-length protein (data not shown). Of note, the deletion of the APY repeats at the C terminus extremity of the protein did not affect the enzyme specificity and efficiency, as previously observed with the alternansucrase and inulosucrase (39, 41).
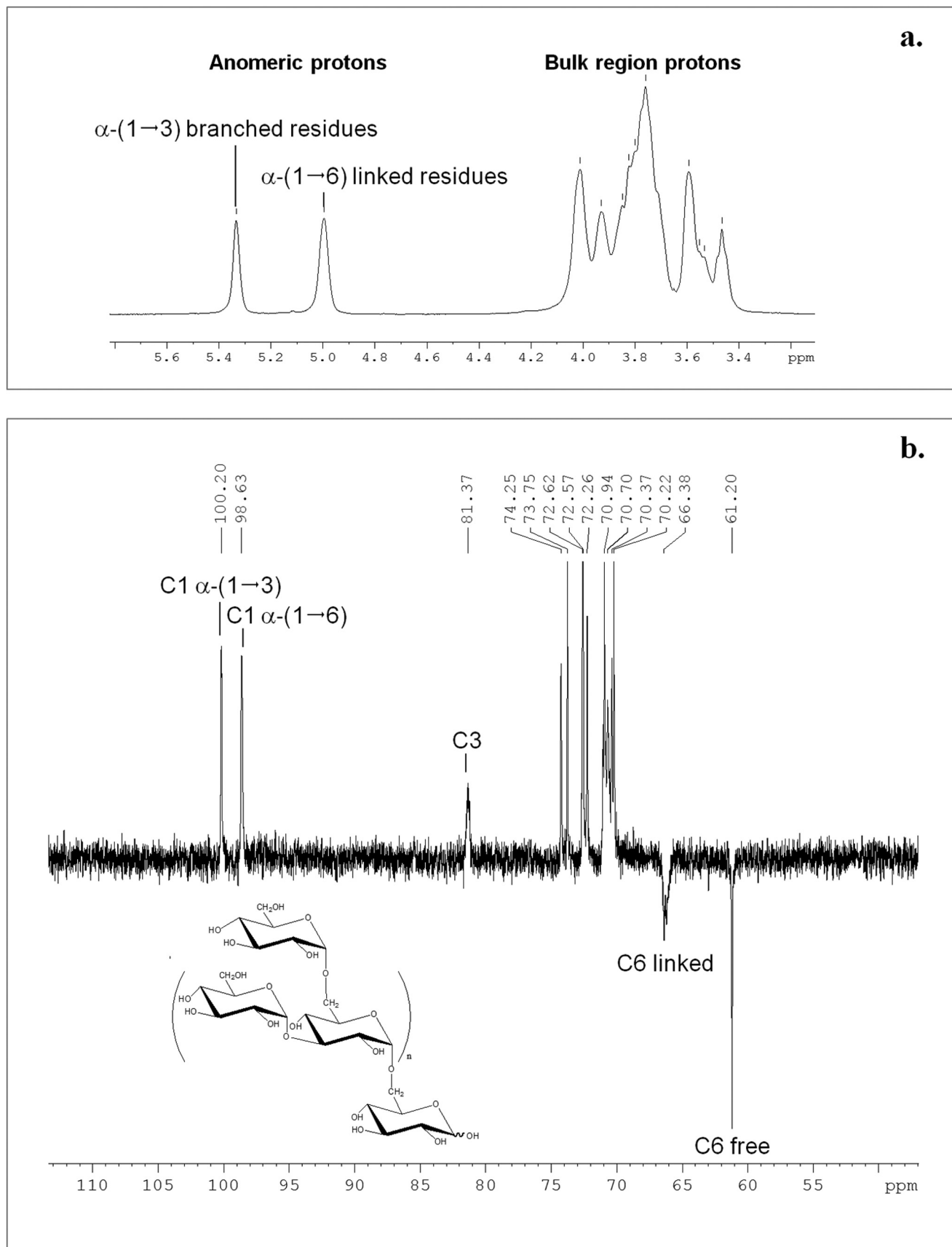
FIGURE 4. **^{1}H NMR (*a*) and ^{13}C NMR (*b*) analyses of the purified branched dextran of 2 × 10^6 g·mol^{-1} synthesized by BRS-B.** ^{13}C chemical shifts are given using acetone as reference (^{13}C = 31.08 ppm).
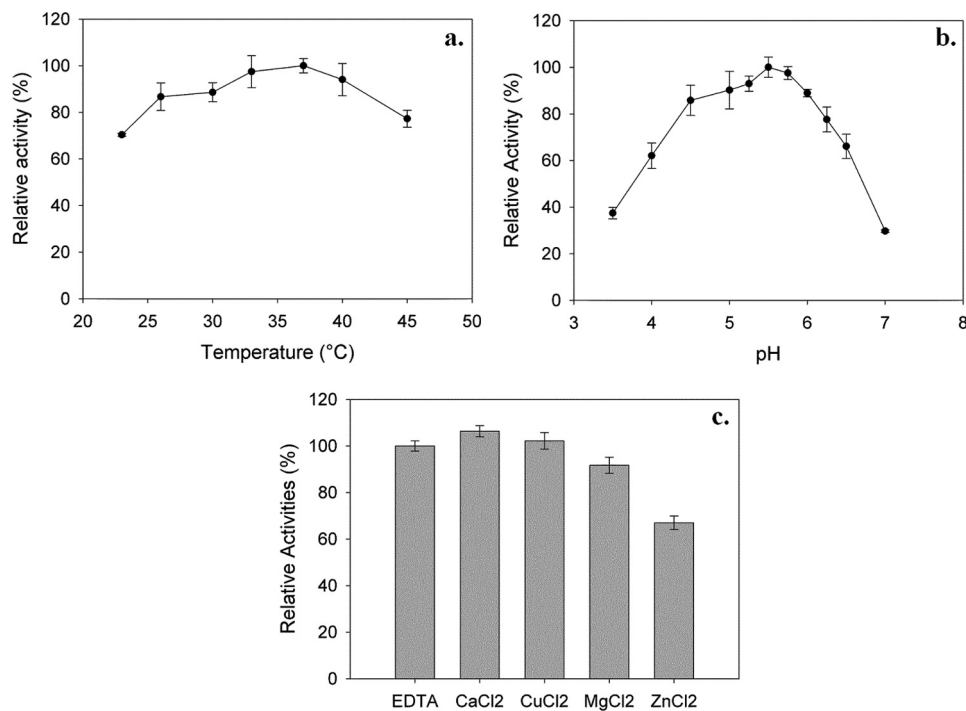
FIGURE 5. **Effect of temperature (*a*), pH (*b*), and the addition of divalent ions (*c*) on BRS-B-Δ1 transferase activity.** Results are given as the means ± S.D. *n* = 3.

The kinetic parameters of the recombinant protein BRS-B-Δ1 were determined with and without dextran acceptor. Without the acceptor, sucrose hydrolysis was inhibited by >150 mM sucrose, and the kinetic data fitted a non-competitive substrate inhibition modeled by Equation 1 with a K_m, K_i, and k_{cat} values estimated at 7.0 ± 0.7 mM, 595 ± 88 mM, and at 81.4 s^{-1}, respectively. An initial rate of transglucosylation was determined at a fixed sucrose concentration (300 mM) and using dextran acceptor (68,400 g·mol^{-1}) concentrations varying from 31 to 617 mM (in anhydroglucosyl unit equivalents). A classical Michaelis-Menten profile was obtained with K_m dextran and k_{cat} values of 0.27 ± 0.08 mM and 949 s^{-1}, respectively. A 12-fold increase of the catalytic constant was observed compared with the reaction without dextran (Table 2). The formation of α-(1→3) branches onto dextran molecules is very efficient ($k_{cat}/K_{mdextran}$ = 3514 s^{-1} mM^{-1}), and the k_{cat} value is close to that reported for α-(1→2) branching formation catalyzed by the α-(1→2) branching sucrase GBD-CD2 (20) (Table 2). Such values range among the highest k_{cat} values reported for GH70 members.

Synthesis of Dextrans with Controlled Amounts of α-(1→3) Linkages—The opportunity to synthesize different α-glucan structures with a controlled degree of branching using BRS-B-Δ1 was investigated in more details. To this end, low and high molar mass dextrans (1500 and 2 × 10^6 g·mol^{-1}, respectively) were tested as acceptors at different sucrose:acceptor ratios. When sucrose was in large excess, the production yields of α-(1→3)-branched dextrans decreased in favor of the formation of side products (mainly glucose and leucrose, production of small oligosaccharides being negligible). In contrast, when the dextran concentration increased, glucose and leucrose production was reduced (Fig. 6a). The percentage of α-(1→3) link-

ages in branched dextrans was tightly controlled and evolved from 5 to 50% by adjusting the sucrose:acceptor ratio (Fig. 6b). This parameter was also shown to be critical for controlling the percentage of α-(1→2) branching catalyzed by the α-(1→2) branching sucrase, GBD-CD2 (20). An initial sucrose/dextran ratio higher than three has to be used to obtain a highly branched dextran. By controlling the sucrose:acceptor ratio and the size of the dextran acceptor, a large array of products can be produced, opening the possibility of new applications for these kinds of molecules.

Comparison of BRS-B with Other Branching Sucrases and Glucansucrases—The four functional sequence signatures (motifs I-IV), usually well conserved in the GH70 family and also found in related the GH13 family (10), were aligned with the corresponding motifs found in the characterized GH70 enzymes from other organisms (Table 3). Interestingly, BRS-B exhibits numerous sequence similarities with GBD-CD2 and BRS-A from *L. citreum* NRRL B-1299, two branching sucrases (19, 21). In particular, Phe-675 of motif II and Ile-783, His-785, Lys-789, and Val-795 of motif IV are only conserved in the branching sucrases. They are not found in other GH70 conserved motifs and could thus be suggested to be important for branching activity. Other amino acids are uniquely found in BSR-B. They include residues 673-IS of motif II, 711-PKGE of motif 796-IH of motif IV, and F1184 of motif I (Table 3).

The three-dimensional model of BRS-B was constructed by homology modeling using ΔN$_{123}$-GBD-CD2 branching sucrase as template (Fig. 7). The model was compared with the 3D-structures of ΔN$_{123}$-GBD-CD2 (PDB: 3TTQ) and with the inactive mutant of GTF-180-ΔN in complex with sucrose substrate (PDB: 3HZ3). According to the model, BRS-B also adopts a U-shape fold organized in five domains. As shown in Fig. 7,

TABLE 2

Kinetic parameters of truncated variant BRS-B-Δ1 for hydrolysis reaction (in the presence of sucrose) and for α-(1→3) transglucosylation (in the presence of sucrose and dextran 68.4 kg. mol⁻¹)

Comparison with the kinetic parameters of GBD-CD2 and ΔN₁₂₃-GBD-CD2 is shown.

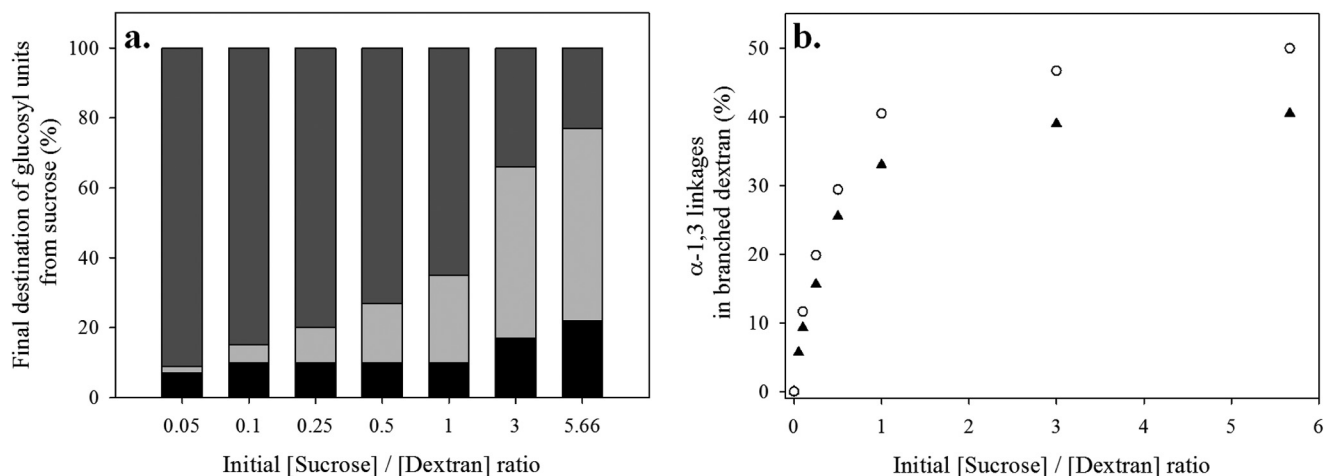| Enzyme	$K_{m\ sucrose}$	$K_{m\ dex}$	$K_{m\ dex}$	V_{max}	k_{cat}
	mM	mM of anhydroglucosyl units	mM	$\mu mol\ mg^{-1}\ min^{-1}$	s^{-1}
Sucrose					
BRS-B−Δ1	7.0 ± 0.7			34.5 ± 1.1	81.4
ΔN₁₂₃-GBD-CD2	7.5 ± 1.0			36.3 ± 0.6	76
GBD-CD2	10.8 ± 0.8			34.6 ± 0.5	109
Sucrose and dextran (68.4 kg·mol⁻¹)					
BRS-B−Δ1		112 ± 33	0.27 ± 0.08	402 ± 36	949
ΔN₁₂₃-GBD-CD2	206 ± 34	125 ± 21	0.3 ± 0.05	462 ± 45	947
GBD-CD2	42 ± 2	75 ± 3	0.174	303 ± 5	970

FIGURE 6. Synthesis of α-(1→3)-branched dextrans using BRS-B-Δ1 and varying sucrose:acceptor initial ratio (mass concentrations). *a*, determination of the percentage of glucosyl moieties from sucrose incorporated into free glucose (*black*), leucrose (*light gray*), and α-(1→3) dextran (*dark gray*). The production of other oligosaccharides was negligible. *b*, control of the amount of α-(1→3) linkages in branched dextrans of 1500 (▲) and 2 × 10⁶ g·mol⁻¹ (○) as the function of the sucrose:acceptor initial ratio.

TABLE 3

Sequence alignment of the conserved motifs (I–IV) of BRS-C and BBRS-D catalytic core with other characterized GH70 enzymes

Enzyme		Motif II		Motif III		Motif IV		Motif I	Spe[1]
GTF-I [Sd] [2,3]	449	SIRVDAVDNVD	486	HVSIVEAWSDN	559	FARAHDSEVQDLIRD	931	ADWVPDQ	M
GTF-B [Sm]	1011	SIRVDAVDNVD	1048	HLSILEAWSDN	1120	FIRAHDSEVQDLIAD	1488	ADWVPDQ	
GTF-A [Lr]	1020	SVRVDAPDNID	1056	HINILEDWNHA	1128	FVRAHDNNSQDQIQN	1508	ADWVPDQ	R
GTF-O [Lr]	1020	SVRVDAPDNID	1056	HINILEDWNSS	1128	FIRAHDNNSQDQIQN	1508	ADWVPDQ	
ASR [Lm]	631	GIRVDAVDNVD	668	HLSILEDWNGK	762	FVRAHDYDAQDPIRK	1168	ADWVPDQ	A
GTF-W [Lr]	748	GFRVDAADNID	785	HLVYNEGYHSG	568	FVTNHDQR-KNVINQ	1216	EDLVMNQ	4,6 GT
GTF-ML4 [Lr]	1012	GFRVDAADNID	1049	HLSYNEGYHSG	1121	FVTNHDQR-KNLINR	1479	EDIVMNQ	
GTF-180 [Lr]	1021	GIRVDAVDNVD	1058	HINILEDWGWD	1131	FVRAHDSNAQDQIRQ	1503	ADWVPDQ	D
DSR-S [Lm]	547	GIRVDAVDNVD	584	HLSILEDWSHN	657	FVRAHDSEVQTVIAQ	1023	ADWVPDQ	
GBD-CD₂ [Lc]	2206	SIRIDAVDFIH	2243	HISLVEAGLDA	2317	IIHAHDKGVQEKVGA	2688	ADVVDNQ	BS
BRS-A [Lc]	668	SIRIDAVDFVS	705	HLSLVEAGLDA	779	IIHAHDKDIQDKVGA	1151	ADVVANQ	
BRS-B [Lc]	667	SMRIDAISFVD	704	HISIVEAPKGE	783	IVHAHDKDIQDTVIH	1182	ADFVANQ	This work
BRS-C [Lf]	734	SIRIDAISFVD	771	HVSIVEASADQ	845	IVHAHDKDIQDAVSN	1232	ADYVANQ	
BRS-D [LbK]	520	SIRIDAVDFIS	557	HISLVEGGVDA	638	IVHAHDKDVQEKVGQ	1010	ADVVYNQ	

[1] Spe, Specificity. Enzymes are grouped together according to their linkage specificity: M for mutansucrase, R for reuteransucrase, A for alternansucrase, 4,6 GT for α-4,6 glucanotransferase, D for dextransucrase, BS for branching sucrase.

[2] The two catalytic residues are indicated in bold red the nucleophile (D) and the acid/base catalyst (E). The transition state stabilizer (D) is represented in bold blue. The residues in bold green and in bold orange correspond to residues of substrate binding subsites −1 and +1, respectively, as originally identified in GTF180-ΔN: sucrose complex (PDB entry 3HZ3) (15).

[3] [Sd] *Streptococcus downei*, [Sm], *Streptococcus mutans*, [Lr], *Lactobacillus reuteri*, [Lm], *L. mesenteroides*, [Lc], *L. citreum*.
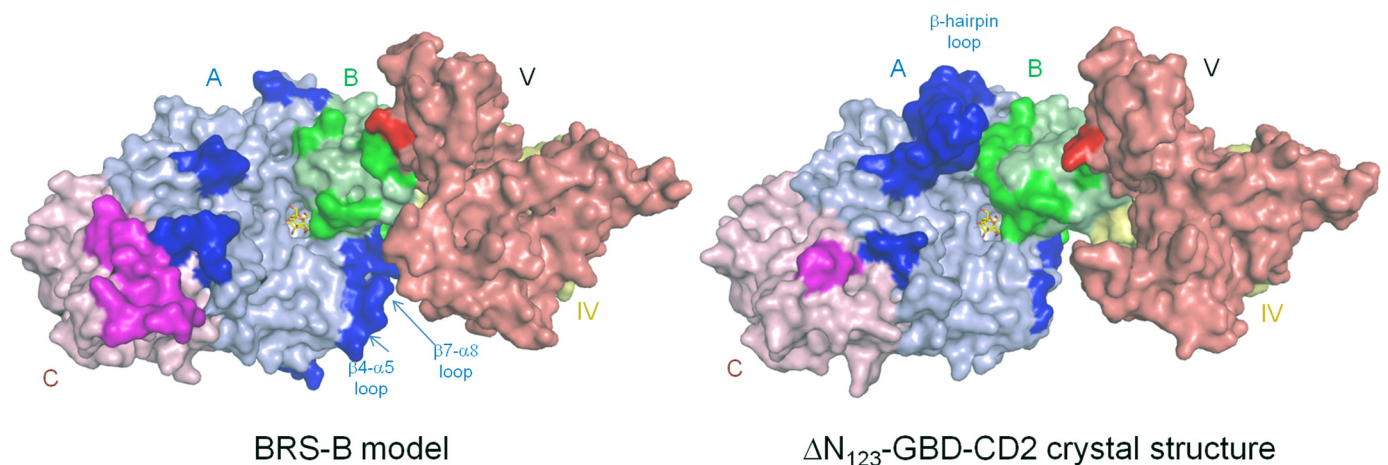
FIGURE 7. Surface representation of BRS-B model and ΔN₁₂₃-GBD-CD2 crystal structure (PDB code 3TTQ). Domains A, B, C, IV, and V are colored in *light blue*, *green*, *pink*, *yellow*, and *red*, respectively. Variable loop regions are shown in bright colors. Sucrose is shown in the active site as *yellow* and *red sticks* for carbon and oxygen atoms, respectively.
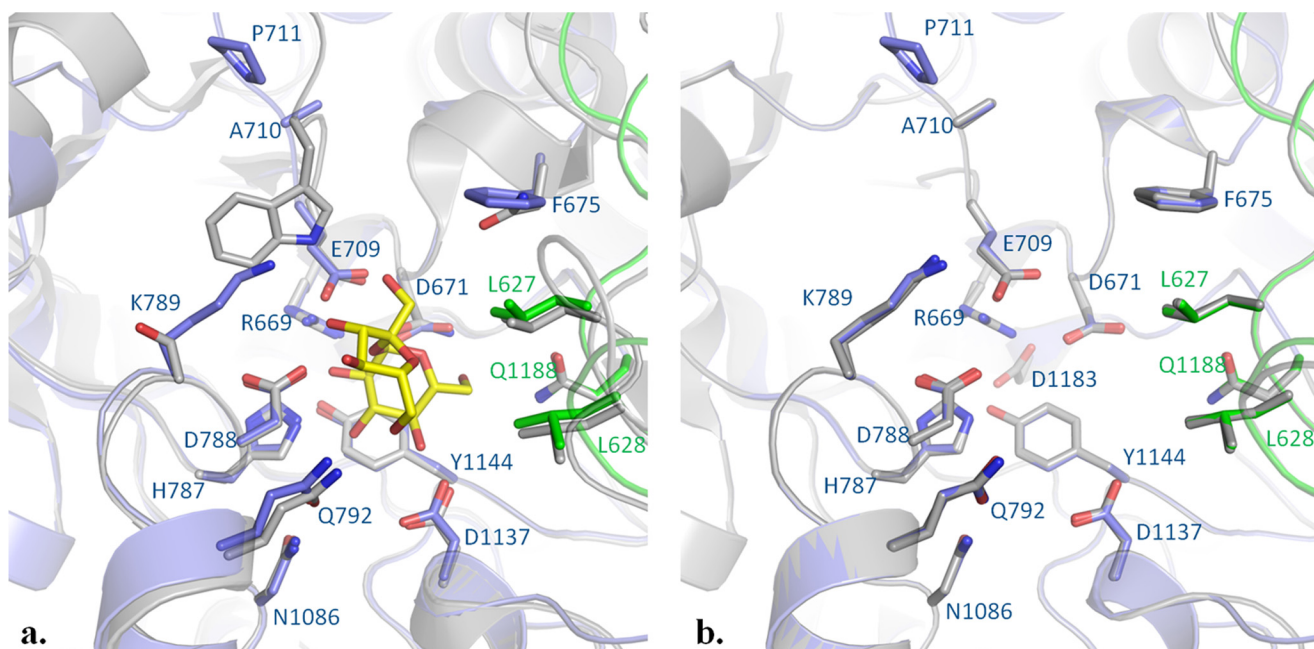

FIGURE 8. Comparison of the active sites of BRS-B, ΔN₁₂₃-GBD-CD2 (PDB code 3TTQ) and GTF-180-ΔN glucansucrase (PDB code 3HZ3). *a*, superimposition of BRS-B with GTF-180-ΔN in complex with sucrose (PDB code 3HZ3). Side chains forming the subsites −1 and +1 are shown as *sticks*. Sucrose is depicted as *yellow* and *red sticks*. GTF-180-ΔN is represented in *gray*, whereas domains A and B of BRS-B are represented in *blue* and *green*, respectively. *b*, superimposition of BRS-B with ΔN₁₂₃-GBD-CD2 structure (PDB code 3TTQ). ΔN₁₂₃-GBD-CD2 is represented in *gray*. Domain A and domain B of BRS-B are represented in *blue* and *green*, respectively.

the BRS-B model displays loops in the vicinity of the catalytic gorge, which differs in length and amino acid composition in comparison with ΔN₁₂₃-GBD-CD2. Of note, the β-hairpin loop partly covering the domain A of ΔN₁₂₃-GBD-CD2 is absent in BRS-B. Near the subsite +1, two loops that belong to the domain B are shorter than in ΔN₁₂₃-GBD-CD2 (G2130-W2135 and Q2158-F2163). In addition, in the catalytic gorge, the two loops connecting strand β4 to helix α5 and strand β7 to helix α8 of the (β/α)₈ barrel are longer in BRS-B.

Then, we compared the active site residues delineating the subsites −1 and +1 of BRS-B with those of GTF-180-ΔN and ΔN₁₂₃-GBD-CD2. As shown in Fig. 8, the residues of subsite −1 are all conserved. In subsite +1, BRS-B and ΔN₁₂₃-GBD-CD2 only differ by one residue: P711 is replaced by G2250 in ΔN₁₂₃-

GBD-CD2. In contrast, only a few residues constituting subsite +1 of GTF-180-ΔN are conserved in BRS-B (*i.e.* Q792, D788 and E709, BRS-B numbering). In particular, N1029 and W1065 of GTF-180-ΔN are not conserved in BRS-B. N1029 is replaced by Phe-675 (Fig. 8*a*). Notably, one phenylalanine was also found in ΔN₁₂₃-GBD-CD2, and was shown to be critical for dextran branching (12). Moreover, comparison of BRS-B and GTF-180 backbone, also revealed a rearrangement around residues A710 and P711 that was observed in ΔN₁₂₃-GBD-CD2. This rearrangement was previously suggested to be responsible for a weaker binding of the fructosyl ring in branching sucrases (12). The identification of the determinants for α-(1→3) branching specificity remains difficult in the absence of three-dimensional structures of BRS-B in apo form or in complex with sucrose or

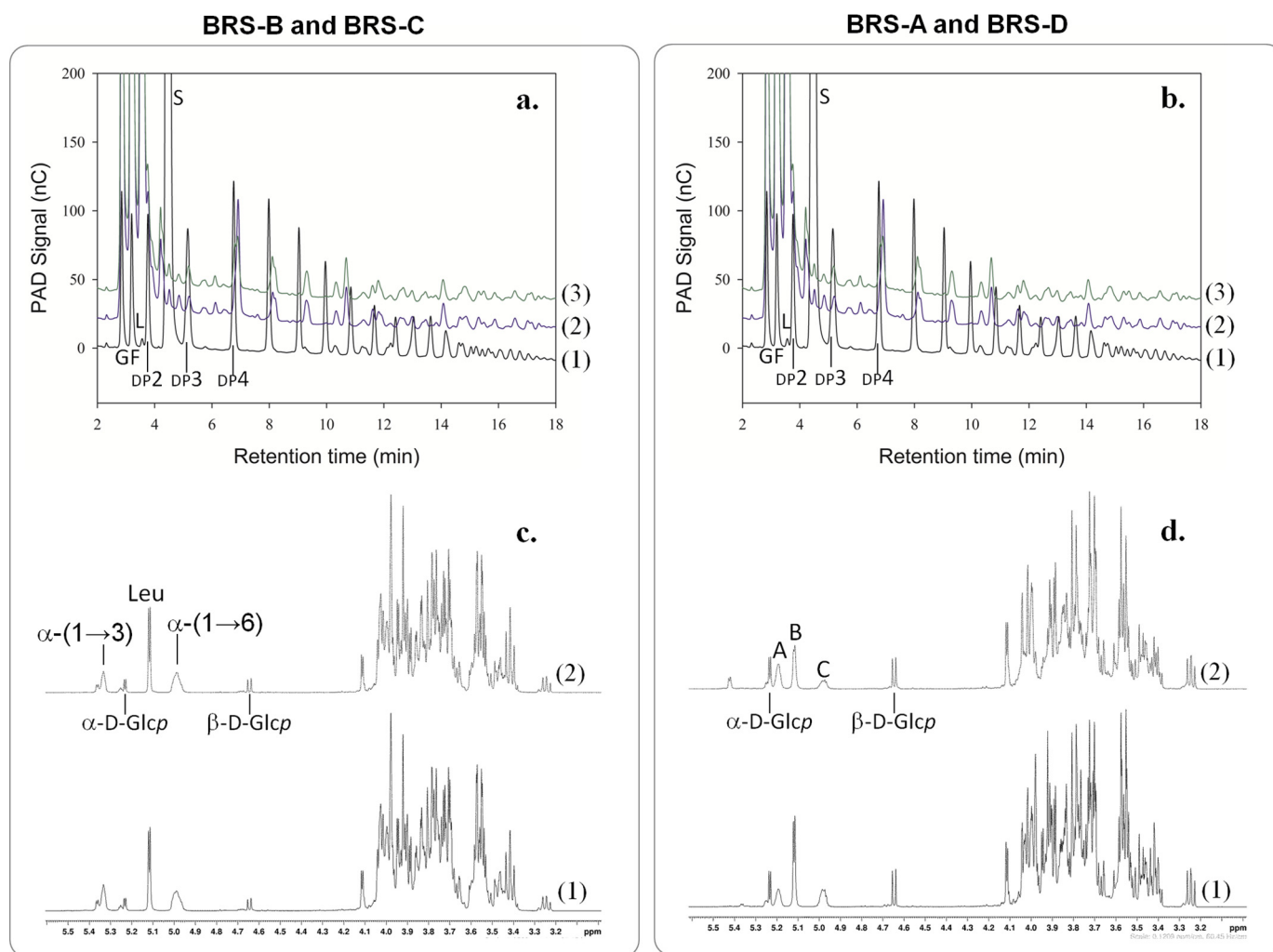FIGURE 9. **Analysis of the products synthesized using BRS-C and BRS-D enzymes from sucrose (292 mM) and dextran 1500 g·mol^{-1} (66.6 mM).** *a,* comparison of BRS-B and BRS-C HPAEC-PAD chromatograms. *(1)* Enzymatic reaction at the initial time (*t* = 0 min), *(2)* enzymatic reaction using BRS-B stopped after 8 h, and *(3)* enzymatic reaction using BRS-C stopped after 8 h. *nC,* nanocoulombs. *b,* comparison of BRS-A and BRS-D HPAEC-PAD chromatograms. *(1)* Enzymatic reaction at the initial time (*t* = 0 min), *(2)* enzymatic reaction using BRS-A stopped after 8 h, and *(3)* enzymatic reaction using BRS-C stopped after 8 h. *G,* peak corresponding to glucose fructose (*F*), leucrose (*L*), sucrose (*S*), and isomaltooligosaccharides with a degree of polymerization (*DP*) of *x*. *c,* ^{1}H NMR spectrum of the products synthesized by BRS-B (*1*) and BRS-C (*2*) at 500 MHz in D$_2$O leucrose (*Leu*), α-D-glucose (α-D-*Glcp*), β-D-glucose (β-D-*Glcp*), α-(1→6)-linked glucosyl residues (α-(1→6)), and α-(1→3)-linked glucosyl residues (α-(1→3)). *d,* ^{1}H NMR spectrum of the products synthesized by BRS-A (*1*) and BRS-D (*2*) at 500 MHz in D$_2$O. The ^{1}H NMR spectra of the BRS-A modified dextran displayed all the chemical shift characteristics of α-(1→2)-branched dextran. The anomeric region of the spectrum contained three main resonances corresponding, respectively, to anomeric resonance of α-(1→6)-linked D-Glcp residues of the main linear chain with free carbon 2 (4.98 ppm, *peak C*), to anomeric resonance from α-(1→6)-linked D-Glcp residues of the main linear chain, with the carbon 2 involved in an α-(1→2) linkage with a branched glucosyl unit (5.18 ppm, *peak A*), to anomeric resonance from α-(1→2)-linked D-Glcp (5.11 ppm, branching points, *peak B*).

dextran. However, according to the structural comparison of branching enzymes and polymerases, amino acids can be pointed out that constitute interesting targets for mutation to assess their role in the α-(1→3) branching specificity.

Searching for New Branching Sucrases in Public Databases— The emergence of natural branching activities through the isolation and characterization of BRS-A (21) and BRS-B in *L. citreum* raised the question of the representation of such type of activity in lactic acid bacteria clade. To shed some light on this issue, a blast search against public sequence databases were carried out to ascertain which sequences contain the residues uniquely conserved in branching enzyme catalytic cores. Two new putative branching sucrases (renamed BRS-C and BRS-D) were identified, one in *Leuconostoc fallax* KCTC3537 and the other in *Lactobacillus kunkeei* EFB6. The percentage of amino

acid identity and similarity with BRS-A and BRS-B is detailed in supporting information (supplemental Table S2), and the alignment of the conserved motifs is presented in Table 3. Based on the sequence alignment, the two putative branching sucrases are predicted to possess the catalytic triad DED and the five structural domains, A, B, C, IV, and V, specific to the GH70 family enzymes (supplemental Fig. S2). Similar to the characterized BRS-A (21) and BRS-B, YG repeats (36) were mainly identified at the N-terminal extremity of the protein. All newly identified genes encoding putative branching sucrases are located on the reverse strand of their genome, as previously observed for *brsA* in *L. citreum* NRRL B-1299 genome (21) and *brsB* in *L. citreum* NRRL B-742 genome. All of them are organized in tandem with another putative glucansucrase (supplemental Fig. S3).
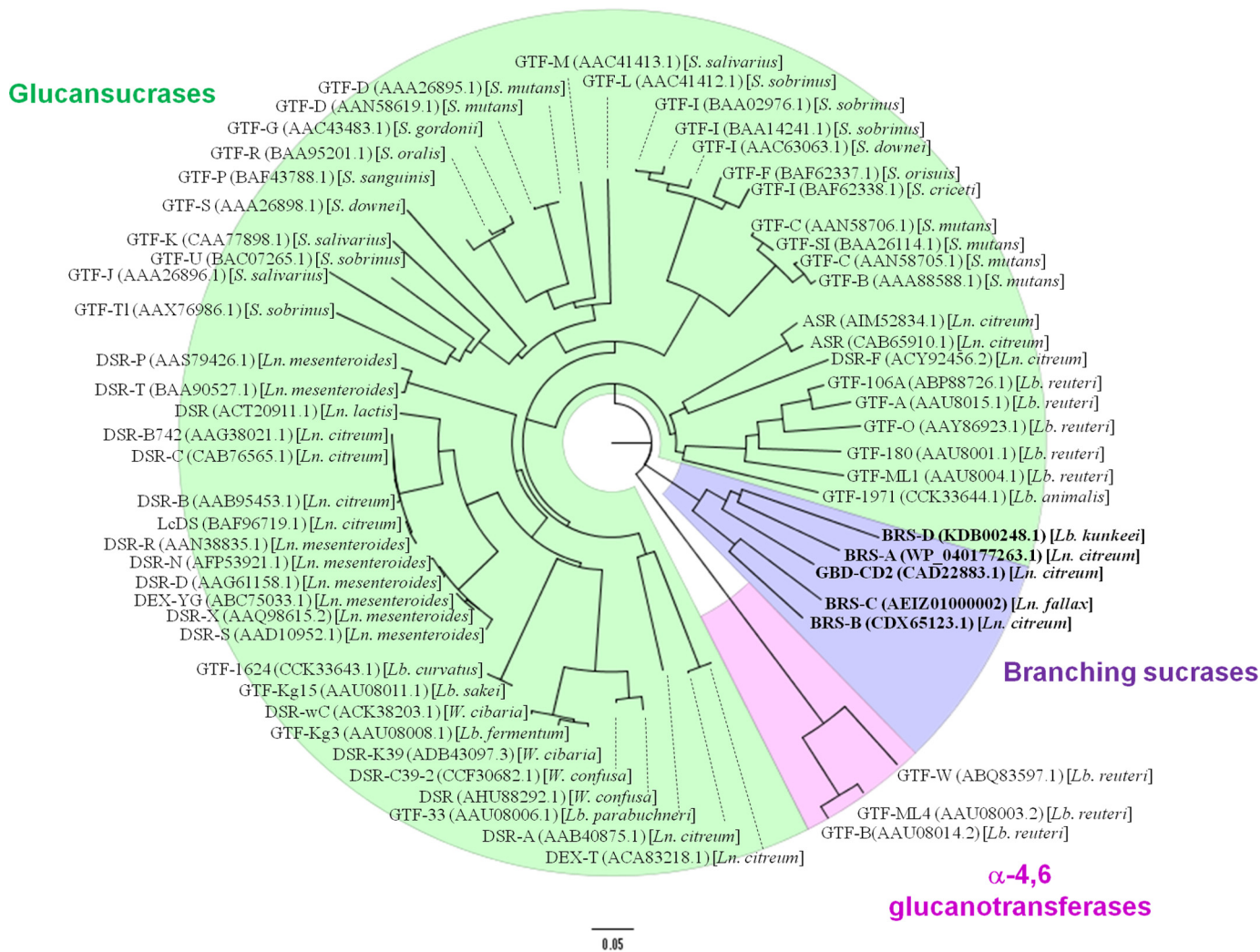
FIGURE 10. **Phylogenetic tree of GH70 enzymes.** Each enzyme is labeled with its GenBank™ accession number and its origin. The species of microorganism are indicated with *Ln.* for *Leuconostoc*, *Lb.* for *Lactobacillus*, *S.* for *Streptococcus*, and *W.* for *Weissella*. Glucansucrase enzymes are highlighted in *green*, α-4,6 glucanstransferases are in *pink*, and branching sucrases are in *bold* and *purple*. The *scale bar* corresponds to a genetic distance of 0.05 substitutions per position.

Characterization of Two New Putative Branching Sucrases and Phylogenetic Analysis—The genes encoding the putative branching sucrases were expressed in *E. coli*. The production levels of the two new proteins are reported in supplemental Table S3. As already observed for BRS-A, BRS-B, and GBD-CD2, the putative BRS-C and BRS-D mainly produced glucose, leucrose, and a low proportion of small oligosaccharides from sucrose substrate (for detailed production yields, see supplemental Table S4). Acceptor reactions were then performed using sucrose and a small dextran of 1500 g·mol⁻¹ as an acceptor. At the end of the reaction, HPAEC-PAD and H¹ NMR analyses demonstrated that dextran was modified by BRS-C and BRS-D (Fig. 9). BRS-C from *L. fallax* KCTC 3537 catalyzed α-(1→3) transglucosylation from sucrose to dextrans, whereas BRS-D from *L. kunkeei* EFB6 was specific for α-(1→2) transglucosylation. These findings reveal for the first time that the branching specificity is not restricted to *L. citreum* sp. but is also present in *L. fallax* as well as in *L. kunkeei*. Interestingly, the phylogenetic analyses show that the branching sucrases cluster together in a distinct branch (Fig. 10). In addition, the branching sucrase subtree is divided into two subgroups,

one corresponding to enzymes showing an α-(1→2) linkage specificity and the other to enzymes with α-(1→3) linkage specificity.

The discovery of the new branching sucrases expands the natural repertoire of the characterized GH70 α-transglucosylases. For years the GH70 family has been mainly known to house glucansucrases. Recently, a new subgroup was disclosed that contains 4,6-α glucanotransferases, a type of α-transglucosylases that uses α-(1→4)-linked glucans as a donor instead of sucrose (42, 43). According to our biochemical and phylogenetic analyses, branching sucrases could also constitute a new GH70 subgroup. Five enzymes of this group have now been characterized, including the engineered α-(1→2) branching sucrase GBD-CD2 (19, 20), BRS-A (21), BRS-B, BRS-C, and BRS-D.

The route is now opened to promising structure-function relationship studies that will aim at identifying the structural determinants responsible for polymerization or branching ability and linkage specificity. Despite common structural motifs with GH70 glucansucrases, the branching sucrases also display clear distinctive features. According to sequence analyses, dif-

References

1. Hucker, G., and Perderson, C. (1930) Studies on the coccaceae. XVI. The genus Leuconostoc. *Tech. Bull. N. Y. Agric Exp. Stn. 167*

2. Van Tieghem, P. (1878) On sugar-mill gum. *Ann. Sci. Nat. Bot. Biol. Végétales.* **7,** 180–203

3. De Belder, A. (2003) *Dextran*, AA Editions, Handbook Amersham Biosciences

4. Bounaix, M.-S., Gabriel, V., Morel, S., Robert, H., Rabier, P., Remaud-Siméon, M., Gabriel, B., and Fontagné-Faucher, C. (2009) Biodiversity of exopolysaccharides produced from sucrose by sourdough lactic acid bacteria. *J. Agric. Food Chem.* **57,** 10889–10897

5. Côté, G. L., and Robyt, J. F. (1983) The formation of α-D-(1→3) branch linkages by an exocellular glucansucrase from *Leuconostoc mesenteroides* NRRL B-742. *Carbohydr. Res.* **119,** 141–156

6. Jeanes, A., and Seymour, F. R. (1979) The α-D-glucopyranosidic linkages of dextrans: comparison of percentages from structural analysis by periodate oxidation and by methylation. *Carbohydr. Res.* **74,** 31–40

7. Remaud, M., Paul, F., Monsan, P., Lopez-Munguia, A., and Vignon, M. (1992) Characterization of α-(1→3) branched oligosaccharides synthesized by acceptor reaction with the extracellular glucosyltransferases from *L. mesenteroides* NRRL B742. *J. Carbohydr. Chem.* **11,** 359–378

8. Robyt, J. F. (1985) *Encyclopedia of Polymer Science*, (Kroschwitz, J. I., ed) Wiley VCH, New York

9. Seymour, F. K., Knapp, R. D., Chen, E. C. M., Bishop, S. H., and Jeanes, A. (1979) Structural analysis of *Leuconostoc* dextrans containing 3-O-α-D-glucosylated α-D-glucosyl residues in both linear-chain and branch-point positions, or only in branch-point positions, by methylation and by ^{13}C NMR spectroscopy. *Carbohydr. Res.* **74,** 41–62

10. Leemhuis, H., Pijning, T., Dobruchowska, J. M., van Leeuwen, S. S., Kralj, S., Dijkstra, B. W., and Dijkhuizen, L. (2013) Glucansucrases: three-dimensional structures, reactions, mechanism, α-glucan analysis, and their implications in biotechnology and food applications. *J. Biotechnol.* **163,** 250–272

11. Lombard, V., Golaconda Ramulu, H., Drula, E., Coutinho, P. M., and Henrissat, B. (2014) The carbohydrate-active enzymes database (CAZy) in 2013. *Nucleic Acids Res.* **42,** 490–495

12. Brison, Y., Pijning, T., Malbert, Y., Fabre, É., Mourey, L., Morel, S., Potocki-Véronèse, G., Monsan, P., Tranier, S., Remaud-Siméon, M., and Dijkstra, B. W. (2012) Functional and structural characterization of a-1,2 branching sucrase derived from DSR-E glucansucrase. *J. Biol. Chem.* **287,** 7915–7924

13. Ito, K., Ito, S., Shimamura, T., Weyand, S., Kawarasaki, Y., Misaka, T., Abe, K., Kobayashi, T., Cameron, A. D., and Iwata, S. (2011) Crystal structure of glucansucrase from the dental caries pathogen *Streptococcus mutans. J. Mol. Biol.* **408,** 177–186

14. Pijning, T., Vujičić-Žagar, A., Kralj, S., Dijkhuizen, L., and Dijkstra, B. W. (2012) Structure of the α-1,6/α-1,4-specific glucansucrase GTFA from *Lactobacillus reuteri* 121. *Acta Crystallogr. Sect. F Struct. Biol. Cryst. Commun.* **68,** 1448–1454

15. Vujicic-Zagar, A., Pijning, T., Kralj, S., López, C. A., Eeuwema, W., Dijkhuizen, L., and Dijkstra, B. W. (2010) Crystal structure of a 117-kDa glucansucrase fragment provides insight into evolution and product specificity of GH70 enzymes. *Proc. Natl. Acad. Sci.* **107,** 21406–21411

16. Moulis, C., Joucla, G., Harrison, D., Fabre, E., Potocki-Veronese, G., Monsan, P., and Remaud-Simeon, M. (2006) Understanding the polymerization mechanism of glycoside-hydrolase family 70 Glucansucrases. *J. Biol. Chem.* **281,** 31254–31267

17. Mooser, G., Hefta, S. A., Paxton, R. J., Shively, J. E., and Lee, T. D. (1991) Isolation and sequence of an active-site peptide containing a catalytic aspartic acid from two *Streptococcus sobrinus* α-glucosyltransferases. *J. Biol. Chem.* **266,** 8916–8922

18. MacGregor, E. A., Jespersen, H. M., and Svensson, B. (1996) A circularly permuted α-amylase-type α/β-barrel structure in glucan-synthesizing glucosyltransferases. *FEBS Lett.* **378,** 263–266

19. Fabre, E., Bozonnet, S., Arcache, A., Willemot, R.-M., Vignon, M., Monsan, P., and Remaud-Simeon, M. (2005) Role of the two catalytic domains of DSR-E dextransucrase and their involvement in the formation of highly α-1,2 branched dextran. *J. Bacteriol.* **187,** 296–303

20. Brison, Y., Fabre, E., Moulis, C., Portais, J.-C., Monsan, P., and Remaud-Siméon, M. (2010) Synthesis of dextrans with controlled amounts of α-1,2 linkages using the transglucosidase GBD-CD2. *Appl. Microbiol. Biotechnol.* **86,** 545–554

21. Passerini, D., Vuillemin, M., Ufarté, L., Morel, S., Loux, V., Fontagné-Faucher, C., Monsan, P., Remaud-Siméon, M., and Moulis, C. (2015) Inventory of the GH70 enzymes encoded by *Leuconostoc citreum* NRRL B-1299: identification of three novel α-transglucosylases. *FEBS J.* **282,** 2115–2130

22. Jeanes, A., Haynes, W. C., Wilham, C. A., Rankin, J. C., Melvin, E. H., Austin, M. J., Cluskey, J. E., Fisher, B. E., Tsuchiya, H. M., and Rist, C. E. (1954) Characterization and classification of dextrans from ninety-six strains of bacteria1b. *J. Am. Chem. Soc.* **76,** 5041–5052

23. Chung, C. H., and Day, D. F. (2004) Efficacy of *Leuconostoc mesenteroides* (ATCC 13146) isomaltooligosaccharides as a poultry prebiotic. *Poult. Sci.* **83,** 1302–1306

24. Chung, C.-H., and Day, D. F. (2002) Glucooligosaccharides from *Leuconostoc mesenteroides* B-742 (ATCC 13146): a potential prebiotic. *J. Ind. Microbiol. Biotechnol.* **29,** 196–199

25. Kim, D., and Robyt, J. F. (1995) Production, selection, and characteristics of mutants of *Leuconostoc mesenteroides* B-742 constitutive for dextransucrases. *Enzyme Microb. Technol.* **17,** 689–695

26. Kim, H., Kim, D., Ryu, H. J., and Robyt, J. F. (2000) Cloning and sequencing of the α-1-> 6 dextransucrase gene from *Leuconostoc mesenteroides* B-742CB. *J. Microbiol. Biotechnol.* **10,** 559–563

27. Passerini, D., Vuillemin, M., Laguerre, S., Amari, M., Loux, V., Gabriel, V., Robert, H., Morel, S., Monsan, P., Gabriel, B., Fontagné-Faucher, C., Remaud-Simeon, M., and Moulis, C. (2014) Complete genome sequence of *Leuconostoc citreum* strain NRRL B- 742. *Genome Announc.* **2,** e01179–14

28. Studier, F. W. (2005) Protein production by auto-induction in high-density shaking cultures. *Protein Expr. Purif.* **41,** 207–234

29. Miller, G. L. (1959) Use of dinitrosalicylic acid reagent for determination of reducing sugar. *Anal. Chem.* **31,** 426–428

30. Irague, R., Massou, S., Moulis, C., Saurel, O., Milon, A., Monsan, P., Remaud-Siméon, M., Portais, J.-C., and Potocki-Véronèse, G. (2011) NMR-based structural glycomics for high-throughput screening of carbohydrate-active enzyme specificity. *Anal. Chem.* **83,** 1202–1206

31. Edgar, R. C. (2004) MUSCLE: multiple sequence alignment with high accuracy and high throughput. *Nucleic Acids Res.* **32,** 1792–1797

32. Biasini, M., Bienert, S., Waterhouse, A., Arnold, K., Studer, G., Schmidt, T., Kiefer, F., Cassarino, T. G., Bertoni, M., Bordoli, L., and Schwede, T.

(2014) SWISS-MODEL: modelling protein tertiary and quaternary structure using evolutionary information. *Nucleic Acids Res.* **42,** W252–W258

33. Fraga Vidal, R., Moulis, C., Escalier, P., Remaud-Siméon, M., and Monsan, P. (2011) Isolation of a gene from *Leuconostoc citreum* B/110–1-2 encoding a novel dextransucrase Enzyme. *Curr. Microbiol.* **62,** 1260–1266

34. Monchois, V., Willemot, R.-M., Remaud-Simeon, M., Croux, C., and Monsan, P. (1996) Cloning and sequencing of a gene coding for a novel dextransucrase from Leuconostoc mesenteroides NRRL B-1299 synthesizing only α(1–6) and α(1–3) linkages. *Gene* **182,** 23–32

35. Bozonnet, S., Dols-Laffargue, M., Fabre, E., Pizzut, S., Remaud-Simeon, M., Monsan, P., and Willemot, R.-M. (2002) Molecular characterization of DSR-E, an α-1,2 linkage-synthesizing dextransucrase with two catalytic domains. *J. Bacteriol.* **184,** 5753–5761

36. Giffard, P. M., and Jacques, N. A. (1994) Definition of a fundamental repeating unit in streptococcal glucosyltransferase glucan-binding regions and related sequences. *J. Dent. Res.* **73,** 1133–1141

37. Argüello-Morales, M. A., Remaud-Simeon, M., Pizzut, S., Sarçabal, P., Willemot, R., and Monsan, P. (2000) Sequence analysis of the gene encoding alternansucrase, a sucrose glucosyltransferase from *Leuconostoc mesenteroides* NRRL B-1355. *FEMS Microbiol. Lett.* **182,** 81–85

38. Janecek, S., Svensson, B., and Russell, R. R. (2000) Location of repeat elements in glucansucrases of *Leuconostoc* and *Streptococcus* species. *FEMS Microbiol. Lett.* **192,** 53–57

39. Joucla, G., Pizzut, S., Monsan, P., and Remaud-Simeon, M. (2006) Construction of a fully active truncated alternansucrase partially deleted of its carboxyl-terminal domain. *FEBS Lett.* **580,** 763–768

40. Maina, N. H., Tenkanen, M., Maaheimo, H., Juvonen, R., and Virkki, L. (2008) NMR spectroscopic analysis of exopolysaccharides produced by *Leuconostoc citreum* and *Weissella confusa. Carbohydr. Res.* **343,** 1446–1455

41. Olivares-Illana, V., López-Munguía, A., and Olvera, C. (2003) Molecular characterization of inulosucrase from *Leuconostoc citreum*: a fructosyltransferase within a glucosyltransferase. *J. Bacteriol.* **185,** 3606–3612

42. Kralj, S., Grijpstra, P., van Leeuwen, S. S., Leemhuis, H., Dobruchowska, J. M., van der Kaaij, R. M., Malik, A., Oetari, A., Kamerling, J. P., and Dijkhuizen, L. (2011) 4,6-α-Glucanotransferase, a novel enzyme that structurally and functionally provides an evolutionary link between glycoside hydrolase enzyme families 13 and 70. *Appl. Environ. Microbiol.* **77,** 8154–8163

43. Leemhuis, H., Dijkman, W. P., Dobruchowska, J. M., Pijning, T., Grijpstra, P., Kralj, S., Kamerling, J. P., and Dijkhuizen, L. (2013) 4,6-α-Glucanotransferase activity occurs more widespread in *Lactobacillus* strains and constitutes a separate GH70 subfamily. *Appl. Microbiol. Biotechnol.* **97,** 181–193